NeuroImage 146 (2017) 419–428

Contents lists available at ScienceDirect

NeuroImage

journal homepage: www.elsevier.com/locate/neuroimage

The role of the frontal aslant tract and premotor connections in visually guided hand movements

Sanja Budisavljevic[a,b,*], Flavio Dell'Acqua[c], Vera Djordjilovic[d], Diego Miotto[e], Raffaella Motta[e], Umberto Castiello[a,b,f]

[a] Department of General Psychology, University of Padova, 35131 Padova, Italy
[b] Cognitive Neuroscience Center, University of Padova, 35131 Padova, Italy
[c] Natbrainlab, Department of Neuroimaging, Institute of Psychiatry, Psychology and Neuroscience, King's College London, London SE5 8AF, United Kingdom
[d] Department of Statistical Sciences, University of Padova, 35121 Padova, Italy
[e] Department of Medicine, University of Padova, 35131 Padova, Italy
[f] Centro Linceo Interdisciplinare, Accademia Nazionale dei Lincei, 00165 Roma, Italy

ARTICLE INFO

Keywords:
Frontal aslant tract
Premotor connections
Reaching
Grasping
Visuomotor processing
Diffusion imaging tractography

ABSTRACT

Functional neuroimaging and brain lesion studies demonstrate that secondary motor areas of the frontal lobe play a crucial role in the cortical control of hand movements. However, no study so far has examined frontal white matter connections of the secondary motor network, namely the frontal aslant tract, connecting the supplementary motor complex and the posterior inferior frontal regions, and the U-shaped dorsal and ventral premotor fibers running through the middle frontal gyrus. The aim of the current study is to explore the involvement of the short frontal lobe connections in reaching and reach-to-grasp movements in 32 right-handed healthy subjects by correlating tractography data based on spherical deconvolution approach with kinematical data. We showed that individual differences in the microstructure of the bilateral frontal aslant tract, bilateral ventral and left dorsal premotor tracts were associated with kinematic features of hand actions. Furthermore, bilateral ventral premotor connections were also involved in the closing grip phase necessary for determining efficient and stable grasping of the target object. This work suggests for the first time that hand kinematics and visuomotor processing are associated with the anatomy of the short frontal lobe connections.

1. Introduction

Advances in our understanding of visuomotor processing showed that frontal lobe circuits are crucial for generating motor commands for simple hand movements such as reaching and reaching-to-grasp (Jeannerod et al., 1995; Castiello, 2005; Grafton, 2010). Reaching refers to a transport of the hand in space, whereas reach-to-grasp action consists of an additional grasping component, which implies hand shaping according to the target object's physical properties (Jeannerod, 1995).

In addition to the primary motor cortex (M1), secondary motor areas including supplementary motor complex and premotor regions are active during reaching and reach-to-grasp movements (Castiello, 2005; Filimon, 2010). Functional neuroimaging and lesion studies implicate these areas in a variety of motor-related processes, such as initiation, generation and control of voluntary hand movements (supplementary motor complex) (Picard and Strick, 1996; Nachev et al., 2008); visuomotor transformations and generation of finger and hand configurations (ventral premotor cortex, PMv) (Davare et al., 2006; Raos et al., 2006), and planning, control and online monitoring of hand actions (dorsal premotor cortex, PMd) (Begliomini et al., 2007, 2008; Glover et al., 2012).

A dual model of visuomotor processing suggested that PMd and PMv are part of two independent circuits, originating from the posterior parietal cortex, which control the reaching and the grasping components of prehensile movements, respectively (Jeannerod et al., 1995; Matelli and Luppino, 2001). However, this view has been challenged recently, when overlapping PMv and PMd activations were reported for both reaching and grasping actions (Grol et al., 2007; Begliomini et al., 2014, 2015; Fabbri et al., 2014; Tarantino et al., 2014). It was shown that PMv and PMd interact based on the motor planning and online control required, but not on the basis of movement type (Grol et al., 2007; Glover et al., 2012). The importance of the connections between PMv and PMd has been further corroborated by

* Correspondening author at: NeMo Laboratory, Department of General Psychology University of Padova, Via Venezia 8, 35131 Padova.
E-mail address: sanja.budisavljevic@gmail.com (S. Budisavljevic).

http://dx.doi.org/10.1016/j.neuroimage.2016.10.051
Received 11 April 2016; Accepted 31 October 2016
Available online 06 November 2016
1053-8119/

our previous work showing modulation of the PMv-PMd functional connectivity during precision grasping (i.e. index finger-thumb opposition; Begliomini et al., 2015). This is in line with the idea that the most appropriate grip type is selected in PMv (F5 in monkey), and then supplied to PMd (F2 in monkey), whose neurons keep a memory trace of the motor representation in order to continuously update hand configuration and orientation during target acquisition (Raos et al., 2004). This intra-hemispheric cross-talk between PMv and PMd is enabled by the underlying local white matter connections (Grafton, 2010).

Overall, research in monkeys and humans provided a comprehensive view on the cortical control of hand actions, but the underlying white matter received little attention. The likely contribution of the short frontal lobe connections mediating local connectivity is essentially unknown. Our study aims to fill this gap by investigating the hodology of white matter networks connecting secondary motor regions, and their role in reaching and reach-to-grasp movements. Specifically, the frontal aslant tract and the system of short U-shaped premotor fibers running superficially to the frontal aslant tract will be considered.

The frontal aslant tract is among the newly described intralobar frontal tracts that links the cortical nodes of the secondary motor network, possibly enabling PMv-PMd cross-talk. It connects the supplementary motor complex in the dorso-medial frontal regions of the superior frontal gyrus (SFg), and the most posterior part of the Broca's territory (pars opercularis, BA44, pars triangularis, BA45, but also precentral regions, BA6) (Ford et al., 2010; Catani et al., 2012; Thiebaut de Schotten et al., 2012; Vergani et al., 2014). The supplementary motor complex consists of two areas (Nachev et al., 2008), namely the supplementary motor area (SMA) supporting online control, and the pre-SMA responsible for movement planning during reach-to-grasp movements (Glover et al., 2012). The SMA, unlike the pre-SMA, has direct connections to M1 and the spinal cord, and it is thus considered as a premotor area (Dum and Strick, 1991). The frontal aslant tract's ventral terminations lie within PMv, which includes precentral BA6 and Broca's area BA44 (Vogt and Vogt, 1919; Binkofski and Buccino, 2004). Cytoarchitectonically, BA44 represents the most likely human homologue of monkey's F5, crucially involved in hand movements (for reviews see Rizzolatti et al., 2002; Binkofski and Buccino, 2004; Fadiga and Craighero, 2006), such as grasping and other manipulative actions (Binkofski et al., 1999a, 1999b, 2000; Gerardin et al., 2000; Nishitani and Hari, 2000; Grèzes et al., 2003; Hamzei et al., 2003). To date, the frontal aslant tract has been associated with different aspects of speech and language (Catani et al., 2013; Kinoshita et al., 2014; Kronfeld-Duenias et al., 2014; Mandelli et al., 2014; Vassal et al., 2014; Fujii et al., 2015; Kemerdere et al., 2015; Sierpowska et al., 2015) and orofacial movement control in Foix-Chavany-Marie syndrome (Martino et al., 2012), but its contribution to voluntary hand movements remains unknown. In addition, a system of short U-shaped fibers running superficially to the frontal aslant tract has been described, interconnecting SFg and inferior frontal gyrus (IFg) to the posterior portion of the middle frontal gyrus (MFg) (Catani et al., 2012). We use the terms dorsal (MFg-SFg) and ventral (MFg-IFg) premotor connections, having in mind the proposed PMv-PMd border at the level between the superior and inferior frontal sulci in humans (Tomassini et al., 2007). The functions of these premotor U-shaped fibers are unknown. Nevertheless, based on their cortical topography, it was suggested that the dorsal connections might play a role in initiating and coordinating complex eye, hand and arm movements for reaching actions, while the ventral connections may support the 'grasping' network (Catani et al., 2012).

Here we used diffusion imaging tractography, based on the spherical deconvolution approach, to dissociate the role of the short frontal connections underlying secondary motor areas in visually guided hand movements. Spherical deconvolution has the advantage, over the classical diffusion tensor model, to resolve the crossing fibers problem and improve tractography reconstructions of short intralobar tracts by reducing the presence of false negatives (Tournier et al., 2004; Dell'Acqua et al., 2010, 2013). We dissected the frontal aslant tract and the premotor U-shaped connections in 32 right-handed healthy participants, whose hand kinematics was separately recorded for reaching and reach-to-grasp movements. The hindrance modulated orientational anisotropy (HMOA) was used as a measure of white matter microstructure, being a true tract-specific index, and better reflecting the microstructural organization (e.g. myelination, axonal density, axon diameter, and fiber dispersion) than the traditional voxel-specific diffusion indices (e.g. fractional anisotropy) (Dell'Acqua et al., 2013). We hypothesized that individual differences in the microstructure of the short frontal lobe connections linking secondary motor areas would be associated with the kinematic markers of reach and reach-to-grasp movements. Furthermore, according to previous literature outlining the evidence of a crucial involvement of the bilateral PMv in hand shaping and grip formation, we expected to find a higher involvement of the ventral premotor connections in the grasp-specific components of reach-to-grasp actions, compared to the dorsal premotor fibers, expected to be more involved in reaching.

2. Materials and methods

2.1. Participants

A sex and age-balanced sample of 32 healthy participants (14 males, 18 females; mean age 24.6 ± 2.7, age range: 20–31 years) was recruited. All participants were right-handed according to the Edinburgh Handedness Inventory (Oldfield, 1971), which ranges from -100 for purely left handed to +100 for purely right-handed participant. No history of neurological and psychiatric disorders was present in the study sample. All participants gave informed written consent in accordance with the ethics approval by the Institutional Review Board at the University of Padova, in accordance with the Declaration of Helsinki (Sixth revision, 2008).

2.2. Behavioral experiment

2.2.1. Task and stimulus

Participants were requested to perform two tasks: a reach-to-grasp task, in which they were asked to reach toward and grasp the stimulus with a precision grip, and a reaching task in which they were asked to perform a movement toward the stimulus and touch the stimulus frontal surface with their knuckles, maintaining the hand in a closed fist (Fig. 1). The fist's posture was chosen as to minimize distal involvement. Participants fixated the target object during both the reaching and the reach-to-grasp actions. The stimulus consisted of a spherical object (2 cm diameter) that would normally be grasped with a precision grip (PG; using the index finger and thumb). All participants were explicitly asked to use a PG for grasping the object. Participants were informed as to which task to perform by an auditory cue (high-pitch: reach-to-grasp; low-pitch: reaching). The sound also had a 'go-signal' function in the sense that participants were asked to start their actions toward the stimulus only after the sound was delivered. Trials in which the participants did not comply with the task or did not fixate the stimulus were not included in the analysis.

2.2.2. Procedure

Each participant sat on a height-adjustable chair in front of a table (900×900 mm) with the elbow and wrist resting on the table surface and the right hand in the designated start position (Fig. 1). The hand was pronated with the palm resting on a pad (60×70 mm), which was shaped to allow for a comfortable and repeatable posture of all digits, i.e., slightly flexed at the metacarpal and proximal interphalangeal joints. The starting pad was attached 90 mm away from the edge of the table surface. The object was placed on a platform located at a distance

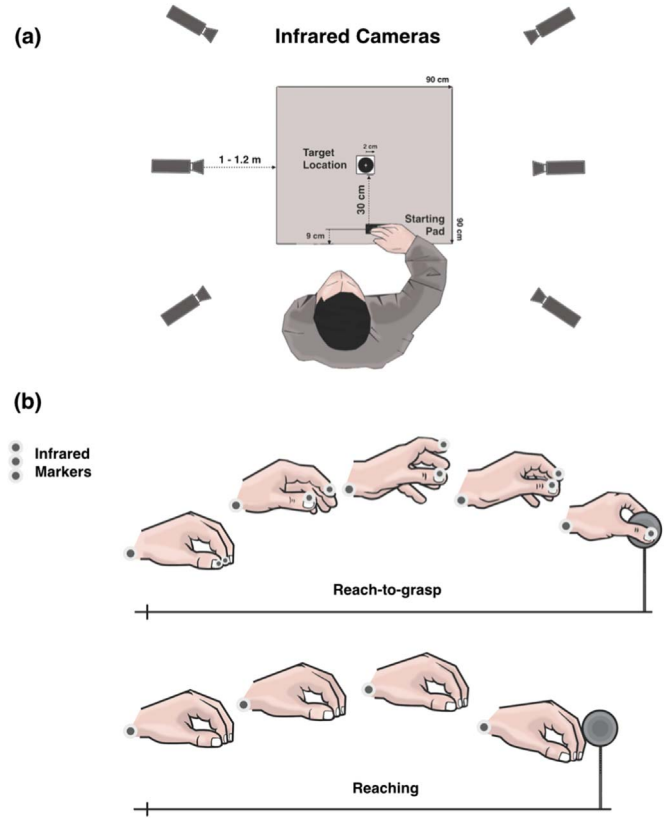

Fig. 1. Descriptive example of the experimental set up showing (a) designated start position for (b) reach-to-grasp and reaching movements.

of 300 mm between the platform and the sagittal plane of the hand's starting position on the right side of the table.

2.2.3. Kinematics recording

A 3D-Optoelectronic SMART-D system (Bioengineering Technology and Systems, BTS) was used to track the kinematics of the participant's right upper limb. Three light-weight infrared reflective markers (0.25 mm in diameter; B|T|S|) were taped to the following points: (i) thumb (ulnar side of the nail); (ii) index finger (radial side of the nail); and (iii) wrist (dorsodistal aspect of the radial styloid process). Six video cameras (sampling rate 140 Hz) detecting the markers were placed in a semicircle at a distance of 1–1.2 m from the table. The camera position, roll angle, zoom, focus, threshold, and brightness were calibrated and adjusted to optimize marker tracking, followed by static and dynamic calibration. For the static calibration, a three-axes frame of five markers at known distances from each other was placed in the middle of the table. For the dynamic calibration, a three-marker wand was moved throughout the workspace of interest for 60 s. The spatial resolution of the recording system was 0.3 mm over the field of view. The standard deviation of the reconstruction error was below 0.2 mm for the x-, y-, and z-axes.

2.2.4. Data processing

Following data collection, each trial was individually checked for correct marker identification and the SMART-D Tracker software package (B|T|S|) was used to provide a 3-D reconstruction of the marker positions as a function of time. The data were then filtered using a finite impulse response linear filter (transition band=1 Hz, sharpening variable=2, cut-off frequency=10 Hz; D'Amico and Ferrigno, 1990, 1992). Movement onset was defined as the time at which the tangential velocity of the wrist marker crossed a threshold (5 mm/s) and remained above it for longer than 500 ms. For the reach-to-grasp task the end of movement was defined as the time at which the hand made contact with the stimulus and quantified as the time at which the hand opening velocity crossed a threshold (-5 mm/s) after reaching its minimum value and remained above it for longer than 500 ms. For the reaching task the end of movement was defined as the time at which the hand made contact with the stimulus and quantified as the time at which the wrist velocity crossed a threshold (5 mm/s) after reaching its minimum value and remained above it for longer than 500 ms. For both reaching and reach-to-grasp tasks the following kinematic parameters were extracted for each individual movement using a custom protocol run in Matlab 2014b (The 4 MathWorks, Natick, MA, USA): the time interval between movement onset and end of movement (Movement Time), the time at which the tangential velocity of the wrist was maximum from movement onset (Time to Peak Wrist Velocity) and its amplitude (Amplitude of Maximum Peak Velocity), the time at which the acceleration of the wrist was maximum from movement onset (Time to Peak Acceleration) and its amplitude (Amplitude of Maximum Peak Acceleration), the time at which the deceleration of the wrist was maximum from movement onset (Time to Peak Deceleration) and its amplitude (Amplitude of Maximum Peak Deceleration). For the reach-to-grasp task three grasp specific measures were also assessed, namely the time at which the distance between the 3D coordinates of the thumb and index finger was maximum, between movement onset and hand contact time (Time to Maximum Grip Aperture); and the time and amplitude of the maximum closing grip velocity.

2.3. MRI data acquisition

Diffusion imaging data was acquired using a Siemens Avanto 1.5 T scanner housed in Padova University Hospital with actively shielded magnetic field gradients (maximum amplitude 45mT/m^{-1}). The body coil was used for RF transmission, and an 8-channel head coil for signal reception. Protocol consisted of a localizer scan, followed by a single-shot, spin-echo, EPI sequence with the following parameters: TR=8500, TE=97, FOV=307.2×307.2, matrix size=128×128, 60 slices (no gaps) with isotropic (2.4×2.4×2.4 mm^3) voxels. The maximum diffusion weighting was 2000 sec/mm^2, and at each slice location 7 images were acquired with no diffusion gradients applied (b=0 s/mm^2), together with 64 diffusion-weighted images in which gradient directions were uniformly distributed in space and repeated 3 times, in order to increase signal to noise ratio (SNR). Gains and scaling factors were kept constant between acquisitions. Scanning lasted approximately 30 min.

2.4. Correction of motion and eddy current distortion, and estimation of the fiber orientation distribution

Each subject's raw image data were examined before proceeding on to further analyses to detect any outliers in the data, including signal drop-outs, poor signal-to-noise ratio, and image artifacts such as ghosts. Any subject whose raw data contained volumes with significant image quality issues was removed from further analyses. The remaining 32 participants were processed as follows.

DWI datasets were concatenated and corrected for subject motion and geometrical distortions using ExploreDTI (http://www.exploredti.com; Leemans et al., 2009), which by default rotates b-vectors. Spherical deconvolution (Tournier et al., 2004, 2007; Dell'Acqua et al., 2007) approach was chosen to estimate multiple orientations in voxels containing different populations of crossing fibers (Alexander, 2005). Spherical deconvolution was calculated applying the damped version of the Richardson-Lucy algorithm with a fiber response parameter α =1.5, 200 algorithm iterations and η=0.15 and ν=15 as threshold and geometrical regularization parameters (Dell'Acqua et al., 2010). Fiber orientation estimates were obtained by selecting the orientation corresponding to the peaks (local maxima) of the Fibre Orientation Distribution (FOD) profiles. FOD is defined as a spherical

function describing for each voxel the total number of distinct fibre orientations, their actual orientations and the estimated density.

2.5. Tractography algorithm

Whole brain tractography was performed selecting every brain voxel with at least one fibre orientation as a seed voxel. To identify the main fibre orientations and exclude spurious local maxima, we applied both an absolute and a relative threshold on the FOD amplitude. The first "absolute" threshold corresponding to a Hindrance Modulated Orientational Anisotropy (HMOA) threshold of 0.015 was used to exclude small FOD local maxima due to noise or partial volume effects with isotropic tissue (Dell'Acqua et al., 2013). This threshold can be considered the equivalent of the FA threshold in classical DTI tractography and is used to select from each FOD only major peaks and exclude low amplitude spurious FOD components derived from noise, grey matter and cerebrospinal fluid contamination and not consistent with real orientations. The second "relative" threshold of 5% of the maximum amplitude of the FOD was applied to check and remove remaining local maxima with values that might be still greater than the absolute threshold but that represent only a small fraction of the overall HARDI signal and therefore still produce spurious or unreliable orientations (Dell'Acqua et al., 2013). In practice, for the large majority of brain voxel the absolute threshold is always the largest of the two thresholds and effectively used as the only threshold.

From each voxel, and for each fiber orientation, streamlines were propagated using a modified Euler integration with a step size of 1 mm. When entering a region with crossing white matter bundles, the algorithm followed the orientation vector of the least curvature. Streamlines were halted when a voxel without fiber orientation was reached or when the curvature between two steps exceeded a threshold of 45°. All spherical deconvolution and tractography processing was performed using StarTrack, a freely available Matlab software toolbox developed by one of the authors (F.D. NatBrainLab, King's College London), and based on the methods described in Dell'Acqua et al. (2013).

2.6. Tractography dissections of the frontal aslant tract and premotor connections

To visualize fibre tracts and quantify tract-specific measures we used TrackVis software (http://www.trackvis.org; Wang et al., 2007). We used two regions of interest (ROIs) approach to isolate the frontal aslant tract and premotor U-shaped tracts connecting the middle frontal gyrus with the inferior (MFg-IFg ventral tract) and superior frontal gyri (MFg-SFg dorsal tract), according to a dissection method previously described in Catani et al. (2012) and Rojkova et al. (2015). Three separate frontal 'AND' ROIs were manually delineated on the FA maps of each subject in each hemisphere. The 'AND' ROI is used to represent an obligatory passage for the tract, and thus includes the desired streamlines passing through it. We delineated on axial slices an 'AND' ROI around the white matter of the superior frontal gyrus (SFg ROI) and a sagittal 'AND' ROI around the white matter of the inferior frontal gyrus (also including the pars opercularis, triangularis and orbitalis) (IFg ROI). Finally an 'AND' ROI was delineated around the white matter of the middle frontal gyrus (MFg ROI) in axial and sagittal sections. Frontal aslant tract was dissected using SFg ROI and IFg ROI; MFg-IFg ventral tract using MFg ROI and IFg ROI, and lastly MFg-SFg dorsal tract was visualized using MFg ROI and SFg ROI. An example of tractography reconstructions in a representative subject, together with the ROIs used, is shown in Fig. 2.

2.7. Statistical analysis

Statistical analysis was performed using SPSS software (Version 21) (SPSS, Chicago, IL). Gaussian distribution was confirmed for kinematic and tractography HMOA variables using the Shapiro–Wilk test (α-level: $p < .05$) (Shapiro and Wilk, 1965) allowing the use of parametric statistics. The mean value for each kinematic parameter of interest was determined based on 12 individual observations for each participant, and then entered into separate paired-samples t-tests for comparing reaching versus reach-to-grasp conditions. To estimate the effect size we calculated Cohen's *d* for dependent t-tests, from formula described in Dunlop et al. (1996, S. 171) - as cited and calculated at: http://www.psychometrica.de/effect_size.html (January 2016).

The mean HMOA was calculated for each tract in each subject, defined as the absolute amplitude of each lobe of the FOD, and representing a quantitative index of the degree of tract anisotropy. HMOA was chosen over fractional anisotropy (FA) as it is considered to be a tract-specific index sensitive to axonal myelination, fiber diameter, and axonal density (Dell'Acqua et al., 2013). The main difference between FA and HMOA is that FA is a traditional voxel-based metrics providing an average measure of anisotropy of the entire voxel derived from fitting the data according to the Diffusion Tensor model. On the contrary, HMOA is a new tract specific metrics based on the Spherical Deconvolution approach. The main advantage of this metric is being able to 1) resolve partial volume contamination of different white matter tracts crossing within the same voxel or brain region and 2) provide a distinct and therefore a more "true" tract-specific quantification of anisotropy and microstructural organization along each white matter tract (i.e. if two fibres are crossing the same voxel, two distinct and independent HMOA values are assigned to each tract) (Dell'Acqua et al., 2013). Pearson bivariate correlation analysis was used to detect the strength of the correlation between the tract-specific HMOA measure and the kinematic markers of reaching and reach-to-grasp movements. We employed a false discovery rate (FDR) correction (Benjamini and Hochberg, 1995) for 102 comparisons using the q-value of 0.05 for significant results (FDR $p < .05$). We used Fisher's r-to-z transformation and asymptotic z-test to statistically test the difference between the two dependent correlations with one variable in common – the amplitude of closing grip velocity (Lee and Preacher, 2013). Degree of manual dominance (mean value 97 ± 6, ranging from +70 to +100) had no significant effect on the measured variables and the correlations reported.

3. Results

3.1. Behavioral results

Means, standard deviations and statistical tests are summarized in Table 1. We explored the determinants of the movement kinematics by comparing the conditions in which the participants were requested to reach towards and grasp the stimulus (reach-to-grasp) or solely reach the stimulus (reaching). For all seven dependent measures a statistically significant effect of the task was found. Reaching was significantly faster than reaching-to-grasp, and the time to peak velocity, acceleration, and deceleration was reached earlier. The amplitude of peak velocity, acceleration and deceleration was higher for the reaching than for the reach-to-grasp task. Time to maximum grip aperture, and time and amplitude of closing grip velocity are grasp-specific measures, shown only for the reach-to-grasp task (Table 1.).

3.2. Group average visualization of the frontal aslant tract and premotor connections

To visualize fibre tracts at a group level, we calculated group average probability maps of the three bilateral frontal lobe connections (see Fig. 3). We first performed elastic transformations to a standard space (MNI) from each subjects' FA maps using FLIRT/FNIRT (FSL software; Jenkinson et al., 2012). Tractography density maps for each tract were then transformed applying the same deformation fields,

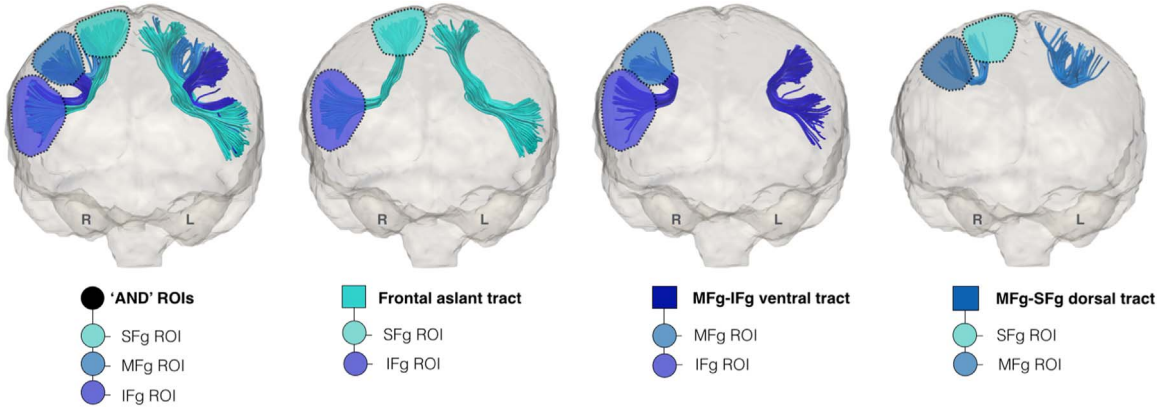

Fig. 2. Tractography reconstructions of the left and right frontal aslant tract (cyan) and U-shaped connections of the middle frontal gyrus with the inferior (MFg-IFg ventral tract; dark blue) and the superior frontal gyri (MFg-SFg dorsal tract; light blue) in a representative subject. Frontal 'AND' ROIs including superior frontal gyrus (SFg ROI), middle frontal gyrus (MFg ROI) and inferior frontal gyrus (IFg ROI) are shown for the right hemisphere, together with the rules employed for the dissection.

Table 1
Movement time and kinematic values showing statistically significant differences between reaching and reach-to-grasp movements. *M*=means, *SD*=standard deviation, *d*=Cohen's *d*.

Variable	*M* ± *SD*		*t* (df)	*d*	*p*
	Reaching	Reach-to-Grasp			
Movement Time (ms)	655 ± 53	733 ± 55	−17.3 (31)	−1.45	< .0001
Time to Peak Velocity (ms)	262 ± 24	308 ± 29	−11.2 (31)	−1.74	< .0001
Time to Peak Acceleration (ms)	165 ± 15	218 ± 19	−15.6 (31)	−3.06	< .0001
Time to Peak Deceleration (ms)	426 ± 30	500 ± 28	−11.5 (31)	−2.56	< .0001
Amplitude Peak Velocity (mm/s)	814 ± 53	698 ± 63	12.7 (31)	1.96	< .0001
Amplitude Peak Acceleration (mm/s^2)	7907 ± 245	6733 ± 480	20.3 (31)	2.38	< .0001
Amplitude Peak Deceleration (mm/s^2)	7507 ± 385	6508 ± 493	15.9 (31)	2.18	< .0001
Time to Maximum Grip Aperture (ms)	n/a	509 ± 22	n/a	n/a	n/a
Time of Closing Grip Velocity (ms)	n/a	684 ± 29	n/a	n/a	n/a
Amplitude of Closing Grip Velocity (mm/s)	n/a	−396 ± 68	n/a	n/a	n/a

binarized and averaged together to generate for each tract a group-averaged probability map ranging from 0 (i.e. no subject has the tract passing through that voxel) to 1 (all subjects have the tract in that voxel).

3.3. Relating inter-individual differences in movement kinematics to the anatomy of the frontal aslant tract and premotor U-shaped connections

3.3.1. Kinematics and the frontal aslant tract

We observed a significant relationship between the white matter microstructure, as measured by HMOA, of the bilateral frontal aslant tract and the acceleration and deceleration amplitudes of both reaching and reach-to-grasp movements (Table 2; Fig. 4). Higher HMOA in the bilateral frontal aslant tract corresponded to lower acceleration and deceleration amplitudes for both hand movements. Before the FDR correction, correlation with the time to peak acceleration of reaching and reaching-to-grasp and the right frontal aslant tract was also significant.

3.3.2. Kinematics and the ventral premotor U-shaped tract

Regarding the ventral U-shaped connections between the middle and inferior frontal gyrus (MFg-IFg), we found significant relationship between this bilateral tract and deceleration amplitudes for reaching movements, and the right ventral premotor tract with the reach-to-grasp movements, with higher HMOA corresponding to lower deceleration amplitudes (Table 2; Fig. 4). Furthermore, the left ventral premotor tract was significantly associated with the acceleration amplitudes, with higher HMOA corresponding to lower acceleration amplitudes in both reaching and reach-to-grasp conditions (Table 2). Lastly, right ventral premotor connections were significantly associated with the grasp component of the reach-to-grasp action, while the left counterpart showed only a trend towards significance after the FDR correction. Higher HMOA corresponded to higher amplitudes of closing grip velocity (Fig. 5). In contrast, the frontal aslant tract and the dorsal premotor connections did not correlate with grasp-specific measures, and this difference was significant. Hence, the correlation with the right ventral tract was significantly different from correlations with the left (z=2.90, *p*=.003) and the right frontal aslant tract (z=2.60, *p*=.009) and the left (z=2.44, *p*=.014) and the right dorsal premotor tract (z=3.01, *p*=.002).

3.3.3. Kinematics and the left dorsal premotor U-shaped tract

We found significant relationship between the left U-shaped dorsal premotor (MFg-SFg) connections and acceleration amplitudes of reaching and reach-to-grasp movements. Also, the left dorsal premotor tract was significantly associated with the deceleration amplitude during reaching, while during reaching-to-grasp it showed only a trend towards significance after the FDR correction. Overall, higher HMOA of the left dorsal premotor tract corresponded to lower amplitudes of acceleration and deceleration (Table 2, Fig. 4). The correlations with the amplitudes of velocity of reach and reach-to-grasp movements showed only a trend towards significance after FDR correction. No significant correlations were found for the right dorsal premotor connections.

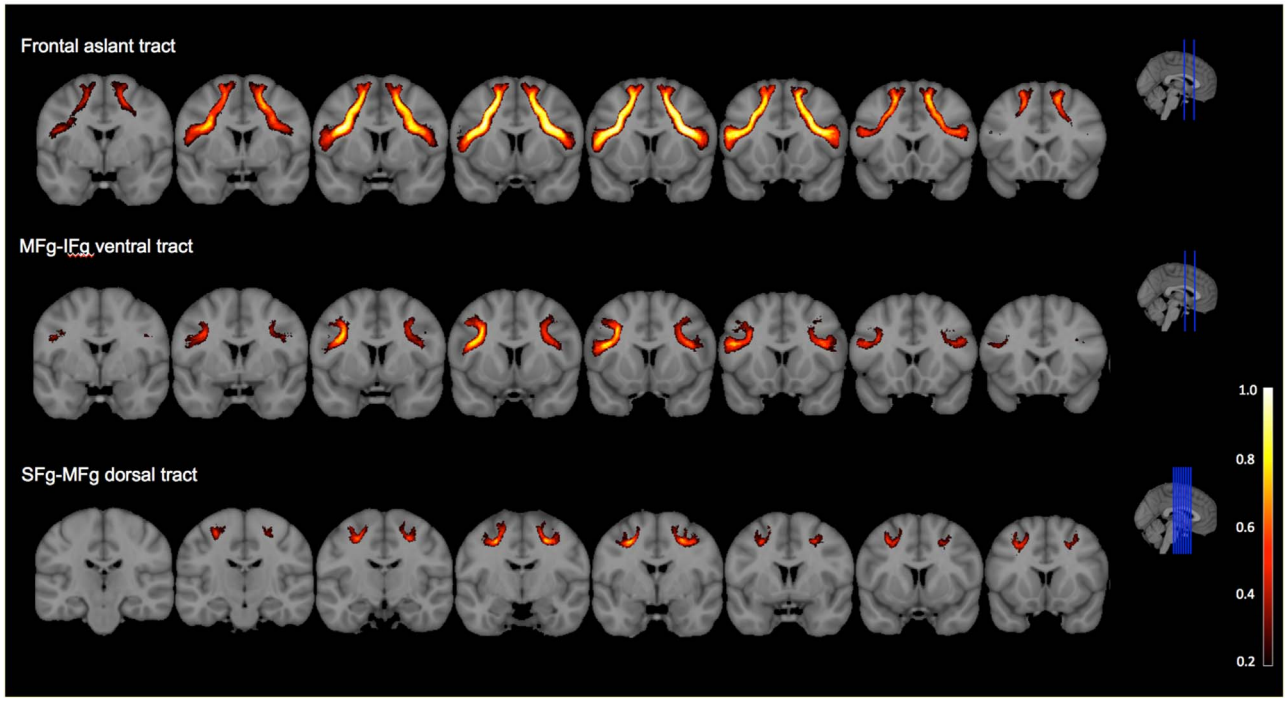

Fig. 3. Group-averaged visualizations of the frontal aslant tract, ventral and dorsal premotor connections. Tracts are displayed when at least 20% of subjects have a tract passing through the same voxel.

Table 2
Correlations between HMOA measure of the frontal aslant tract and the U-shaped connections between the middle and the inferior frontal gyri (MFg-IFg; ventral tract), and the middle and the superior frontal gyri (MFg-SFg; dorsal tract) and kinematic variables, with correlation coefficient estimates and raw *p*-values in brackets. Significance codes show corresponding FDR adjusted p-values at '***' $p < .001$ '**' $p < .01$ '*' $p < .05$ '.' $p < .1$. R: reaching, RG: reach-to-grasp.

Tract		Time to Peak **Acceleration**		Amplitude of Peak **Velocity**		Amplitude of Peak **Acceleration**		Amplitude of Peak **Deceleration**		Amplitude of **Closing Grip Velocity**
		R	**RG**	**R**	**RG**	**R**	**RG**	**R**	**RG**	**RG**
Frontal Aslant Tract	*Left*	−.235 (.195)	.005 (.977)	−.282 (.118)	−.322 (.073)	**−.475*(.007)**	**−.487*(.009)**	**−.625**(< .001)**	**−.550**(.001)**	.107(.575)
	Right	−.420. (.019)	−.433 (.021)	−.397 (.030)	−.325 (.075)	**−.478*(.006)**	−.442.(.013)	**−.620**(< .001)**	**−.521*(.003)**	.124(.521)
MFg-IFg Ventral Tract	*Left*	.009(.962)	.345 (.053)	−.193 (.290)	−.197 (.281)	**−.483*(.005)**	**−.552*(.001)**	**−.745***(< .0001)**	**−.585**(.001)**	.408.(.028)
	Right	−.233 (.208)	.095 (.611)	−.331 (.069)	−.163 (.382)	−.369(.041)	−.337(.064)	**−.558**(.001)**	−.377(.037)	**.521*(.004)**
MFg-SFg Dorsal Tract	*Left*	−.008 (.965)	.302 (.098)	−.443. (.013)	−.405. (.023)	**−.504*(.004)**	**−.560**(.001)**	**−.516*(.003)**	−.395.(.028)	.138(.474)

4. Discussion

This work demonstrates, for the first time, a direct relationship between short frontal lobe connections of the secondary motor areas and the kinematical organization of human upper limb movements. The microstructure of the bilateral frontal aslant tract and the premotor connections was significantly associated with variation in hand kinematics, especially with arm acceleration and deceleration amplitudes for both reaching and reach-to-grasp movements. Our results suggest that these connections might be important for specifying movement trajectory features that relate to dynamic properties of the arm. This might occur by anticipating and accounting for dynamic properties of the proximal limb muscles and the environment (Schaefer et al., 2007; Mani et al., 2013; Mutha et al., 2013). Furthermore, the ventral premotor tract was associated with the closing grip phase during which contact points are determined in order to assure an efficient and stable contact with the target object.

To better understand the role of the frontal lobe for the control of hand actions, we moved on from the relatively detailed knowledge of the cortical motor mechanisms to investigate the role of the corresponding white matter. Recent diffusion imaging studies provide converging evidence that fronto-parietal white matter pathways are a significant determinant of motor performance (Koch et al., 2010; Budisavljevic et al., 2016). Our results extend knowledge on the hodology of motor control (Catani, 2007), and show an important role for the secondary motor white matter networks in hand movements. The bilateral involvement of the frontal aslant tract and ventral premotor U-shaped connections parallels the findings of bilateral secondary motor activations during reaching and grasping movements (Ehrsson et al., 2000; Begliomini et al., 2007, 2015; Martin et al., 2011; for a review see Castiello and Begliomini, 2008).

Our results show that higher microstructural organization of the bilateral frontal aslant tract corresponds to lower acceleration and deceleration amplitudes of reach and reach-to-grasp movements, i.e. more efficient visuomotor processing leading to smoother movement trajectories. The involvement of the frontal aslant tract, connecting

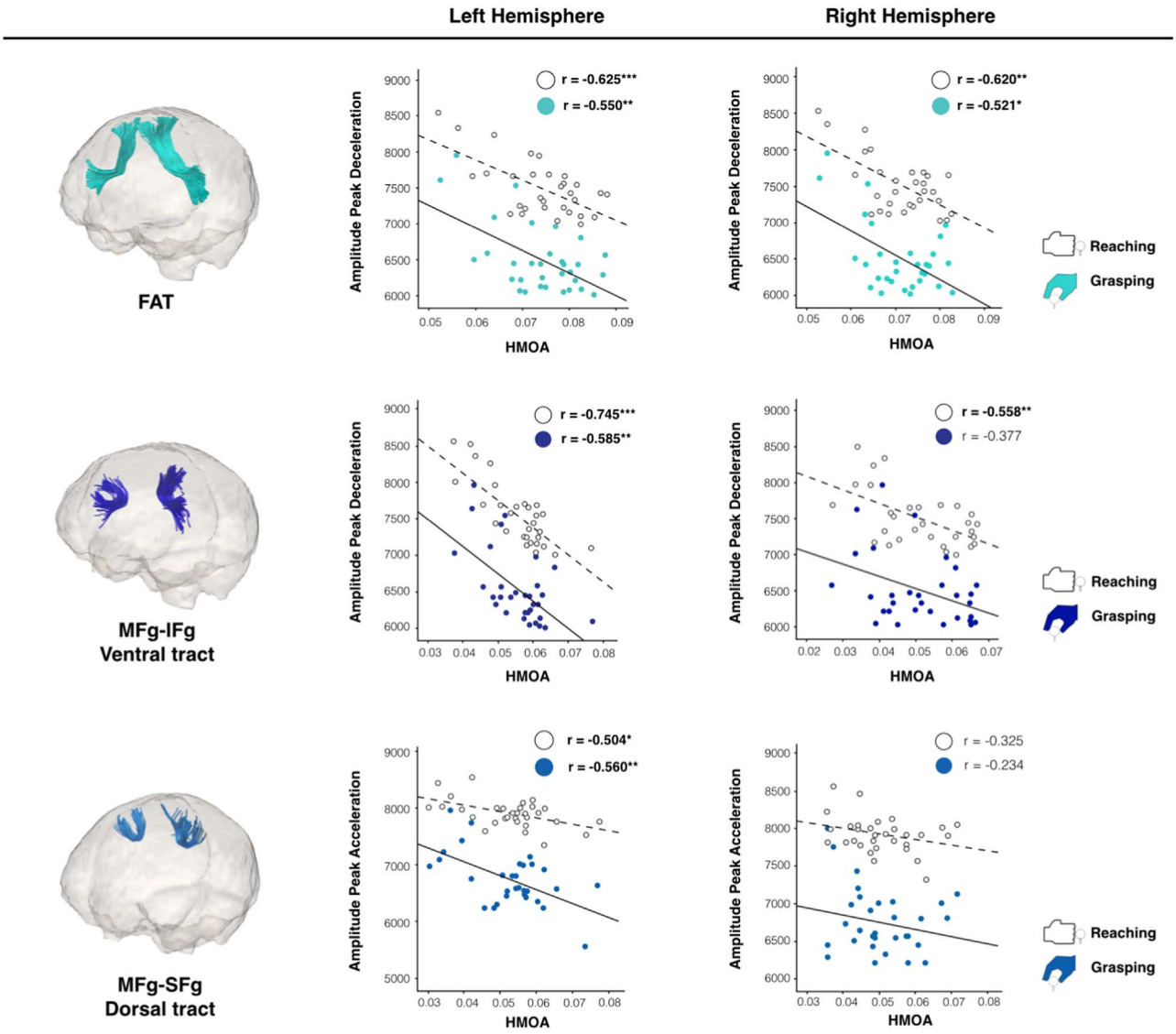

Fig. 4. Correlations between the kinematic variables of reaching and reaching-to-grasp (amplitudes of peak acceleration and deceleration (mm/s^2)) and the HMOA of the frontal aslant tract (FAT; in cyan) and U-shaped tracts (ventral MFg-IFg and dorsal MFg-SFg; in blue) in the left and the right hemisphere. Significance codes represent FDR adjusted p-values: '***' $p < .001$ '**' $p < .01$ '*' $p < .05$.

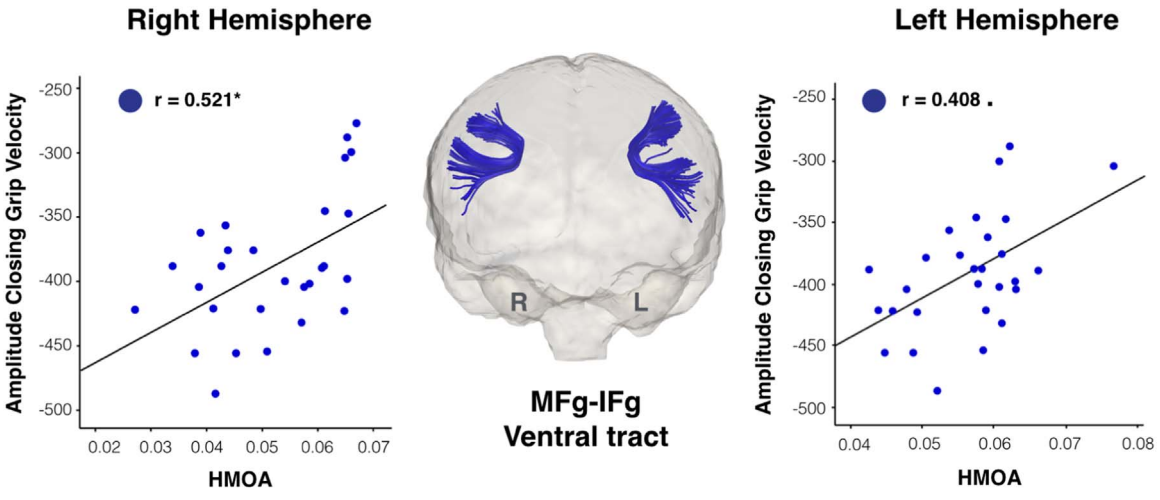

Fig. 5. Correlations between the bilateral ventral premotor (MFg-IFg) U-shaped connections and the grasp-specific measure (amplitude of closing grip velocity; mm/s). Significance codes represent FDR adjusted p-values: '*' $p < .05$ '.' $p < .1$.

portions of the dorsal and ventral promotor cortex (PMd-PMv), is consistent with functional neuroimaging and lesion studies implicating its cortical endpoints in reaching and reach-to-grasp movements. The supplementary motor complex (SMA/pre-SMA) in the dorso-medial frontal lobe is active during hand actions (Grafton et al., 1996; Ehrsson et al., 2000; Cavina-Pratesi et al., 2010; Glover et al., 2012; Monaco et al., 2015); and so is BA44 of the posterior Broca's area (Binkofski et al., 1999a, 1999b, 2000; Ehrsson et al., 2000, 2001; Gerardin et al., 2000; Kuhtz-Buschbeck et al., 2001), the putative homologue of monkey's PMv (F5) where visuomotor transformations of object properties into appropriate hand configurations occur (Rizzolatti et al., 2002). The contribution of the human BA44 to hand movements, in terms of associative sensorimotor learning and sensorimotor integration has been well documented (Rizzolatti et al., 2002; Binkofski and Buccino, 2004; Fadiga and Craighero, 2006). Together with the precentral BA6 regions, BA44 is thought to represent the human PMv (Vogt and Vogt, 1919; Binkofski and Buccino, 2004). The importance of the intra-hemispheric PMd-PMv cross-talk was previously inferred from a number of functional connectivity studies (Crosson et al., 2001; Binkofski et al., 2000; Begliomini et al., 2015). For instance, it has been recently reported that functional connectivity between the human PMd and PMv, corresponding to the frontal aslant fibers, was significantly modulated during reach-to-grasp movements (Begliomini et al., 2015). Also, it was proposed that automatic reach and grasp actions induced by intraoperative cortical stimulation of medial frontal wall areas, including pre-SMA, are due to a release of reach- and grasp-specific motor programs stored in other areas including PMv (Chassagnon et al., 2008). Our results support the notion that the frontal aslant tract underlies the intra-hemispheric cross-talk between PMd and PMv regions, and plays an important role in hand movements.

Another aspect of the present findings is that the bilateral ventral premotor connections were associated with the grasp component of the reach-to-grasp movements. Higher microstructural organization of the bilateral ventral premotor tracts corresponded to higher amplitudes of closing grip velocity, possibly implying more efficient visuomotor processing in terms of finger positioning. We suggest that the ventral premotor connections might be especially important for controlling the final hand closing phase around the target object during precision grip, a complex motor act with a high degree of sensorimotor control (Ehrsson et al., 2000, 2001). Importantly, both the left and the right PMv were found to play a role in precision grasping (Ehrsson et al., 2000, 2001; Dettmers et al., 2003; Davare et al., 2006, 2008; Chouinard, 2006; Raos et al., 2006; Schmidlin et al., 2008) consistent with our results. It was previously suggested that bilateral PMv controls the correct positioning of the fingers upon the object, a prerequisite for an efficient grasp, whereas the left contralateral PMv recruits intrinsic hand muscles (Davare et al., 2006). Our results go beyond the cortical regions, suggesting that the underlying ventral premotor connections in both hemispheres determine grasp point selection for the correct and stable position of the fingers around the target object (Lukos et al., 2007, 2008; Sartori et al., 2011).

On the contrary, it was the left dorsal premotor tract, linking the superior and the middle frontal gyri, that was associated with the dominant right hand kinematics of both reaching and reach-to-grasp movements. The dominance of the left dorsal premotor connections in controlling the right dominant hand is in line with previous studies showing the crucial role of the left, but not the right dorsal premotor cortex (PMd) in precision grasping and sequential hand movements (Haslinger et al., 2002; Hlustik et al., 2002; Davare et al., 2006). Furthermore, its relationship with the proximal limb dynamics and trajectory control (i.e. acceleration and deceleration amplitudes) is consistent with the observation that the left PMd is crucial for the recruitment of proximal muscles of the dominant right hand during precision grasping (Davare et al., 2006), and that it intervenes in coding velocity and acceleration amplitudes during movement preparation (Davare et al., 2015). It is also in line with studies noting that the left hemisphere is important for the control of movement trajectories (Haaland et al., 2004), for sequencing and triggering of sequential movements (Winstein and Pohl, 1995; Hermsdörfer et al., 1999a, 1999b), and for limb dynamics (Tretriluxana et al., 2008; Sainburg and Kalakanis, 2000; Sainburg, 2002; Sainburg and Wang, 2002).

Our study has important implications for the functional correlates of the newly described frontal aslant tract and the U-shaped premotor connections in the human brain. Besides being involved in language (Catani et al., 2013; Kinoshita et al., 2014; Kronfeld-Duenias et al., 2014; Mandelli et al., 2014; Vassal et al., 2014; Fujii et al., 2015) and voluntary movement control of orofacial muscles (Martino et al., 2012), we report that the frontal aslant tract supports visuomotor processing of hand movements such as reaching and reach-to-grasp, important for planning (acceleration phase) and feedback control (deceleration phase) that guides the hand to the target object. It is also possible that the frontal aslant tract could be involved in the inhibition of movement, since it connects the cortical nodes of the bilateral negative motor network: the pre-SMA and the posterior part of the inferior frontal gyrus (Filevich et al., 2012; Mandonnet and Duffau, 2014). This idea is supported by studies showing that unilateral subcortical stimulation of the white matter underneath the dorsal premotor cortex and the supplementary motor area, produces a complete arrest of the movement of both hands (Rech et al., 2014) or movement deceleration (Rutten, 2015). The association between movement deceleration and the bilateral frontal aslant tract noted in our study, could give support to its involvement in the negative motor network.

Our results might have several anatomical interpretations. Higher HMOA of the short frontal lobe tracts corresponded to lower acceleration and deceleration amplitudes of visually guided hand movements, leading to smoother movement trajectories. HMOA is a novel tract-specific index of anisotropy that is sensitive to the underlying white matter microstructure. However, like some other diffusion indices (Beaulieu, 2002), it is not very specific, since it reflects several features of white matter such as myelination, axon density, axon diameter, and fiber dispersion (Dell'Acqua et al., 2013). Variation in any of these features can modulate conduction velocity, refractory time, transmission along an axon, and synchronization of signals across a distributed neuronal network (Johansen-Berg, 2010). Thus, individual differences in any of these properties can impact the motor performance. Nevertheless, as a true tract-specific measure HMOA was shown to be more sensitive than voxel-based fractional anisotropy (FA) index (Dell'Acqua et al., 2013), which in our analysis a posteriori did not yield any significant results. Currently, it is not possible to separate the individual contribution of these white matter components, and hence the interpretation of our correlations is not straightforward. HMOA can decrease with increasing radial diffusivity and the axonal radius, thus, it is possible that increased myelination can also decrease HMOA (Dell'Acqua et al., 2013). Therefore, caution should be taken in interpreting the observed correlations in the context of exact microstructural properties that may contribute to kinematic variation.

Lastly, it should be noted that tractography based on multifiber methods such as spherical deconvolution, can be biased toward false positive reconstructions, and can show artifactual tracts that do not correspond to the real anatomy (Dell'Acqua et al., 2013). To overcome these problems, we used HMOA thresholds as exclusion criteria for seeding, propagating, and stopping tracking. Also, we have visually inspected all the tracts to make sure they conform to their described anatomy. It is still possible that smaller branches of the U-shaped connections were not reconstructed in our dataset, due to the limitation of the spatial resolution. However repeating and averaging the measurements 3 times increased the signal-to-noise ratio. Further studies are needed to replicate our results in a larger data cohort, with the inclusion of functional neuroimaging measures.

5. Conclusions

This study is the first to demonstrate that hand kinematics and visuomotor processing is associated with the anatomy of the short frontal lobe networks. Individual differences in the microstructure of the frontal aslant tract and the U-shaped premotor connections were significantly related to the variation in motor performance, especially the acceleration and deceleration amplitudes of reaching and reach-to-grasp movements. We suggest that these networks support trajectory movement features that relate to dynamic properties of the arm. Furthermore, the ventral premotor tract was involved in the closing grip phase, during which efficient and stable contact points with the target object are determined. We contend that a better understanding of the white matter connections linking secondary motor areas in the context of visually guided hand movements provides important insights into motor organization related to planning and execution of hand actions.

Acknowledgements

This work was supported by a grant from the MIUR (N. 287713), the FP7: REWIRE project and the Progetto Strategico, Università di Padova (N. 2010XPMFW4) to Umberto Castiello. We would like to thank NeMo laboratory (http://nemolaboratory.com) for helpful comments on the manuscript. *Conflict of Interest:* None declared.

References

Alexander, D.C., 2005. Multiple-fiber reconstruction algorithms for diffusion MRI. Ann. NY Acad. Sci. 1064, 113–133.
Beaulieu, C., 2002. The basis of anisotropic water diffusion in the nervous system - a technical review. NMR Biomed. 15 (7-8), 435–455.
Begliomini, C., Caria, A., Grodd, W., Castiello, U., 2007. Comparing natural and constrained movements: new insights into the visuomotor control of grasping. PLoS One 2 (10), e1108.
Begliomini, C., Nelini, C., Caria, A., Grodd, W., Castiello, U., 2008. Cortical activations in humans grasp-related areas depend on hand used and handedness. PLoS One 3 (10), e3388.
Begliomini, C., De Sanctis, T., Marangon, M., Tarantino, V., Sartori, L., Miotto, D., Motta, R., Stramare, R., Castiello, U., 2014. An investigation of the neural circuits underlying reaching and reach-to-grasp movements: from planning to execution. Front. Hum. Neurosci. 8, 676.
Begliomini, C., Sartori, L., Miotto, D., Stramare, R., Morra, R., Castiello, U., 2015. Exploring manual asymmetries during grasping: a dynamic causal modeling approach. Front. Psych. 6, 167.
Benjamini, Y., Hochberg, Y., 1995. Controlling the false discovery rate: a practical and powerful approach to multiple testing. J. R. Stat. Soc. Ser. B (Methodol.), 289–300.
Binkofski, F., Amunts, K., Stephan, K.M., Posse, S., Schormann, T., Freund, H.J., Zilles, K., Seitz, R.J., 2000. Broca's region subserves imagery of motion: a combined cytoarchitectonic and fMRI study. Hum. Brain Mapp. 11, 273–285.
Binkofski, F., Buccino, G., 2004. Motor functions of the Broca's region. Brain Lang. 89, 362–369.
Binkofski, F., Buccino, G., Posse, S., Seitz, R.J., Rizzolatti, G., Freund, H.J., 1999a. A fronto-parietal circuit for object manipulation in man: evidence from an fMRI study. Eur. J. Neurosci. 11, 3276–3286.
Binkofski, F., Buccino, G., Stephan, K.M., Rizzolatti, G., Seitz, R.J., Freund, H.J., 1999b. A parieto-premotor network for object manipulation: evidence from neuroimaging. Exp. Brain Res. 128, 21–31.
Budisavljevic, S., Dell'Acqua, F., Zanatto, D., Begliomini, C., Miotto, D., Motta, R., Castiello, U., 2016. Asymmetry and Structure of the Fronto-Parietal Networks Underlie Visuomotor Processing in Humans. Cereb. Cortex. http://dx.doi.org/10.1093/cercor/bhv348.
Castiello, U., 2005. The neuroscience of grasping. Nat. Rev. Neurosci. 6 (9), 726–736.
Castiello, U., Begliomini, C., 2008. The cortical control of visually guided grasping. Neuroscientist 14 (2), 157–170.
Catani, M., 2007. From hodology to function. Brain 130 (Pt 3), 602–605.
Catani, M., Dell'acqua, F., Vergani, F., Malik, F., Hodge, H., Roy, P., Valabregue, R., Thiebaut de Schotten, M., 2012. Short frontal lobe connections of the human brain. Cortex 48 (2), 273–291.
Catani, M., Mesulam, M.M., Jakobsen, E., Malik, F., Martersteck, A., Wieneke, C., Thompson, C.K., Thiebaut de Schotten, M., Dell'Acqua, F., Weintraub, S., Rogalski, E., 2013. A novel frontal pathway underlies verbal fluency in primary progressive aphasia. Brain 136 (Pt 8), 2619–2628.
Cavina-Pratesi, C., Monaco, S., Fattori, P., Galletti, C., McAdam, T.D., Quinlan, D.J., Goodale, M.A., Culham, J.C., 2010. Functional magnetic resonance imaging reveals the neural substrates of arm transport and grip formation in reach-to-grasp actions in humans. J. Neurosci. 30 (31), 10306–10323.
Chassagnon, S., Minotti, L., Kremer, S., Hoffmann, D., Kahane, P., 2008. Somatosensory, motor, and reaching/grasping responses to direct electrical stimulation of the human cingulate motor areas. J. Neurosurg. 109 (4), 593–604.
Chouinard, P.A., 2006. Different roles of PMv and PMd during object lifting. J. Neurosci. 26 (24), 6397–6398.
Crosson, B., Sadek, J.R., Maron, L., Gökçay, D., Mohr, C.M., Auerbach, E.J., Freeman, A.J., Leonard, C.M., Briggs, R.W., 2001. Relative shift in activity from medial to lateral frontal cortex during internally versus externally guided word generation. J. Cogn. Neurosci. 13 (2), 272–283.
Davare, M., Andres, M., Cosnard, G., Thonnard, J.L., Olivier, E., 2006. Dissociating the role of ventral and dorsal premotor cortex in precision grasping. J. Neurosci. 26 (8), 2260–2268.
Davare, M., Lemon, R., Olivier, E., 2008. Selective modulation of interactions between ventral premotor cortex and primary motor cortex during precision grasping in humans. J. Physiol. 586 (11), 2735–2742.
Davare, M., Zénon, A., Desmurget, M., Olivier, E., 2015. Dissociable contribution of the parietal and frontal cortex to coding movement direction and amplitude. Front. Hum. Neurosci. 9, 241.
Dell'Acqua, F., Rizzo, G., Scifo, P., Clarke, R.A., Scotti, G., Fazio, F., 2007. A model-based deconvolution approach to solve fiber crossing in diffusion-weighted MR imaging. IEEE Trans. Biomed. Eng. 54 (3), 462–472.
Dell'Acqua, F., Scifo, P., Rizzo, G., Catani, M., Simmons, A., Scotti, G., Fazio, F., 2010. A modified damped Richardson-Lucy algorithm to reduce isotropic background effects in spherical deconvolution. Neuroimage 49 (2), 1446–1458.
Dell'Acqua, F., Simmons, A., Williams, S.C., Catani, M., 2013. Can spherical deconvolution provide more information that fiber orientations? Hindrance modulated orientational anisotropy, a true-tract specific index to characterize white matter diffusion. Hum. Brain Mapp. 34 (10), 2464–2483.
Dettmers, C., Liepert, J., Hamzei, F., Binkofski, F., Weiller, C., 2003. A lesion in the ventrolateral premotor cortex causes difficulties in grasping. Aktuel-. Neurol. 30, 247–255.
Dum, R.P., Strick, P.L., 1991. The origin of corticospinal projections from the premotor areas in the frontal lobe. J. Neurosci. 11, 667–689.
Ehrsson, H.H., Fagergren, E., Forssberg, H., 2001. Differential fronto-parietal activation depending on force used in a precision grip task: an fMRI study. J. Neurophysiol. 85 (6), 2613–2623.
Ehrsson, H.H., Fagergren, A., Jonsson, T., Westling, G., Johansson, R.S., Forssberg, H., 2000. Cortical activity in precision- versus power-grip tasks: an fMRI study. J. Neurophysiol. 83 (1), 528–536.
Fabbri, S., Strnad, L., Caramazza, A., Lingnau, A., 2014. Overlapping representations for grip type and reach direction. Neuroimage 94, 138–146.
Fadiga, L., Craighero, L., 2006. Hand actions and speech representation in Broca's area. Cortex 42 (4), 486–490.
Filevich, E., Kühn, S., Haggard, P., 2012. Negative motor phenomena in cortical stimulation: implications for inhibitory control of human action. Cortex 48 (10), 1251–1261.
Filimon, F., 2010. Human cortical control of hand movements: parietofrontal networks for reaching, grasping, and pointing. Neuroscientist 16 (4), 388–407.
Ford, A., McGregor, K.M., Case, K., Crosson, B., White, K.D., 2010. Structural connectivity of Broca's area and medial frontal cortex. Neuroimage 52 (4), 1230–1237.
Fujii, M., Maesawa, S., Motomura, K., Futamura, M., Hayashi, Y., Koba, I., Wakabayashi, T., 2015. Intraoperative subcortical mapping of a language-associated deep frontal tract connecting the superior frontal gyrus to Broca's area in the dominant hemisphere of patients with glioma. J Neurosurg. 122 (6), 1390–1396.
Gerardin, E., Sirigu, A., Lehericy, S., Poline, J.B., Gaymard, B., Marsault, C., Agid, Y., 2000. Partially overlapping neural networks for real and imagined hand movements. Cereb. Cortex 10, 1093–1104.
Grèzes, J., Armony, J.L., Rower, J., Passingham, R.E., 2003. Activations related to "mirror" and "canonical" neurones in the human brain: an fMRI study. NeuroImage 18, 928–937.
Glover, S., Wall, M.B., Smith, A.T., 2012. Distinct cortical networks support the planning and online control of reaching-to-grasp in humans. Eur. J. Neurosci. 35 (6), 909–915.
Grafton, S.T., 2010. The cognitive neuroscience of prehension: recent developments. Exp. Brain Res. 204 (4), 475–491.
Grafton, S.T., Fagg, A.H., Woods, R.P., Arbib, M.A., 1996. Functional anatomy of pointing and grasping in humans. Cereb. Cortex 6 (2), 226–237.
Grol, M.J., Majdandzic, J., Stephan, K.E., Verhagen, L., Dijkerman, H.C., Bekkering, H., Verstraten, F.A., Toni, I., 2007. Parieto-frontal connectivity during visually guided grasping. J. Neurosci. 27 (44), 11877–11887.
Haaland, K.Y., Prestopnik, J.L., Knight, R.T., Lee, R.R., 2004. Hemispheric asymmetries for kinematic and positional aspects of reaching. Brain 127, 1145–1158.
Hamzei, F., Rijntjes, M., Dettmers, C., Glauche, V., Weiller, C., Buchel, C., 2003. The human action recognition system and its relationship to Broca's area: an fMRI study. NeuroImage 19, 637–644.
Haslinger, B., Erhard, P., Weilke, F., Ceballos-Baumann, A.O., Bartenstein, P., Grafin von Einsiedel, H., Schwaiger, M., Conrad, B., BoeckerH, 2002. Therole of lateral premotor-cerebellar-parietal circuits in motor sequence control: a parametric fMRI study. Brain Res. Cogn. Brain Res. 13, 159–168.
Hermsdörfer, J., Laimgruber, K., Kerkhoff, G., Mai, N., Goldenberg, G., 1999a. Effects of unilateral brain damage on grip selection, coordination, and kinematics of ipsilesional prehension. Exp. Brain Res. 128 (1-2), 41–51.
Hermsdörfer, J., Ulrich, S., Marquardt, C., Goldenberg, G., Mai, N., 1999b. Prehension with the ipsilateral hand after unilateral brain damage. Cortex 35 (2), 139–161.
Hlustik, P., Solodkin, A., Gullapalli, R.P., Noll, D.C., Small, S.L., 2002. Functional

lateralization of the human premotor cortex during sequential movements. Brain Cogn. 49, 54–62.
Jeannerod, M., Arbib, M.A., Rizzolatti, G., Sakata, H., 1995. Grasping objects: the cortical mechanisms of visuomotor transformation. Trends Neurosci. 18 (7), 314–320.
Jenkinson, M., Beckmann, C.F., Behrens, T.E., Woolrich, M.W., Smith, S.M., 2012. FSL. Neuroimage 62, 782–790.
Johansen-Berg, H., 2010. Behavioural relevance of variation in white matter microstructure. Curr. Opin. Neurol. 23 (4), 351–358.
Kemerdere, R., de Champfleur, N.M., Deverdun, J., Cochereau, J., Moritz-Gasser, S., Herbet, G., Duffau, H., 2015. Role of the left frontal aslant tract in stuttering: a brain stimulation and tractographic study. J. Neurol. 263 (1), 157–167.
Kinoshita, M., de Champfleur, N.M., Deverdun, J., Moritz-Gasser, S., Herbet, G., Duffau, H., 2014. Role of fronto-striatal tract and frontal aslant tract in movement and speech: an axonal mapping study. Brain Struct. Funct. 220 (6), 3399–3412.
Koch, G., Cercignani, M., Pecchioli, C., Versace, V., Oliveri, M., Caltagirone, C., Rothwell, J., Bozzali, M., 2010. In vivo definition of parieto-motor connections involved in planning of grasping movements. Neuroimage 51 (1), 300–312.
Kronfeld-Duenias, V., Amir, O., Ezrati-Vinacour, R., Civier, O., Ben-Shachar, M., 2014. The frontal alsant tract underlies speech fluency in persistent developmental stuttering. Brain Struct. Funct. 221 (1), 365–381.
Kuhtz-Buschbeck, J.P., Ehrsson, H.H., Forssberg, H., 2001. Human brain activity in the control of fine static precision grip forces: an fMRI study. Eur. J. Neurosci. 14 (2), 382–390.
Leemans A., Jeurissen B., Sijbers J., Jones D., 2009. ExploreDTI: a graphical toolbox for processing, analyzing, and visualizing diffusion MR data. In: Proceedings of the 17th Annual Meeting of International Soc Mag Reson Med 3537, Hawaii, USA.
Lukos, J., Ansuini, C., Santanello, M., 2007. Choice of contact points during multidigit grasping: effect of predictability of object center of mass location. J. Neurosci. 27 (14), 3894–3903.
Lukos, J.R., Ansuini, C., Santanello, M., 2008. Anticipatory control of grasping: independence of sensorimotor memories for kinematics and kinetics. J. Neurosci. 28 (48), 12765–12774.
Nachev, P., Kennard, C., Husain, M., 2008. Functional role of the supplementary and pre-supplementary motor areas. Nat. Rev. Neurosci. 9 (11), 856–869.
Nishitani, N., Hari, R., 2000. Temporal dynamics of cortical representation for action. Proc. Natl. Acad. Sci USA 97 (2), 913–918.
Mani, S., Mutha, P.K., Przybyla, A., Haaland, K.Y., Good, D.C., Sainburg, R.L., 2013. Contralesional motor deficits after unilateral stroke reflect hemisphere-specific control mechanisms. Brain 136 (Pt 4), 1288–1303.
Martino, J., de Lucas, E.M., Ibáñez-Plágaro, F.J., Valle-Folgueral, J.M., Vázquez-Barquero, A., 2012. Foix-Chavany-Marie syndrome caused by a disconnection between the right pars opercularis of the inferior frontal gyrus and the supplementary motor area. J. Neurosurg. 117 (5), 844–850.
Matelli, M., Luppino, G., 2001. Parietofrontal circuits for action and space perception in the macaque monkey. Neuroimage 14 (1 Pt 2), S27–32.
Mandelli, M.L., Caverzasi, E., Binney, R.J., Henry, M.L., Lobach, I., Block, N., Amirbekian, B., Dronkers, N., Miller, B.L., Henry, R.G., Gorno-Tempini, M.L., 2014. Frontal white matter tracts sustaining speech production in primary progressive aphasia. J. Neurosci. 34 (29), 9754–9767.
Mandonnet, E., Duffau, H., 2014. Understanding entangled cerebral networks: a prerequisite for restoring brain function with brain-computer interfaces. Front. Syst. Neurosci. 8, 82.
Martin, K., Jacobs, S., Frey, S.H., 2011. Handedness-dependent and -independent cerebral asymmetries in the anterior intraparietal sulcus and ventral premotor cortex during grasp planning. Neuroimage 57 (2), 502–512.
Monaco, S., Sedda, A., Cavina-Pratesi, C., Culham, J.C., 2015. Neural correlates of object size and object location during grasping actions. Eur. J. Neurosci. 41 (4), 454–465.
Mutha, P.K., Haaland, K.Y., Sainburg, R.L., 2013. Rethinking motor lateralization: specialized but complementary mechanisms for motor control of each arm. PLoS One 8 (3), e58582.
Oldfield, R.C., 1971. The assessment and analysis of handedness: the Edinburgh inventory. Neuropsychologia 9 (1), 97–113.
Picard, N., Strick, P.L., 1996. Motor areas of the medial wall: a review of their location and functional activation. Cereb. Cortex 6, 342–353.
Raos, V., Umiltá, M.A., Gallese, V., Fogassi, L., 2004. Functional properties of grasping-related neurons in the dorsal premotor area F2 of the macaque monkey. J. Neurophysiol. 92 (4), 1990–2002.
Raos, V., Umiltá, M.A., Murata, A., Fogassi, L., Gallese, V., 2006. Functional properties of grasping-related neurons in the ventral premotor area F5 of the macaque monkey. J. Neurophysiol. 95 (2), 709–729.
Rech, F., Herbet, G., Moritz-Gasser, S., Duffau, H., 2014. Disruption of bimanual movement by unilateral subcortical electrostimulation. Hum. Brain Mapp. 35 (7), 3439–3445.
Rizzolatti, G., Fogassi, L., Gallese, V., 2002. Motor and cognitive functions of the ventral premotor cortex. Curr. Opin. Neurobiol. 12 (2), 149–154.
Rojkova, K., Volle, E., Urbanski, M., Humbert, F., Dell'Acqua, F., Thiebaut de Schotten, M., 2015. Atlasing the frontal lobe connections and their variability due to age and education: a spherical deconvolution tractography study. Brain Struct. Funct.. http://dx.doi.org/10.1007/s00429-015-1001-3.
Rutten, G.J., 2015. Speech hastening during electrical stimulation of left premotor cortex. Brain Lang. 141, 77–79.
Sainburg, R.L., 2002. Evidence for a dynamic-dominance hypothesis of handedness. Exp. Brain Res. 142, 241–258.
Sainburg, R.L., Kalakanis, D., 2000. Differences in control of limb dybamics during dominant and nondominant arm reaching. J. Neurophysiol. 83, 2661–2675, (- dodaj).
Sainburg, R.L., Wang, J., 2002. Interlimb transfer of visuomotor rotations: independence of direction and final position information. Exp. Brain Res. 145, 437–447.
Sartori, L., Straulino, E., Castiello, U., 2011. How objects are grasped: the interplay between affordances and end-goals. PLoS One 6 (9), e25203. http://dx.doi.org/10.1371/journal.pone.0025203.
Schaefer, S.Y., Haaland, K.Y., Sainburg, R.L., 2007. Ipsilesional motor deficits following stroke reflect hemispheric specializations for movement control. Brain 130 (Pt 8), 2146–2158.
Schmidlin, E., Brochier, T., Maier, M.A., Kirkwood, P.A., Lemon, R.N., 2008. Pronounced reduction of digit motor responses evoked from macaque ventral premotor cortex after reversible inactivation of the primary motor cortex hand area. J. Neurosci. 28 (22), 5772–5783.
Shapiro, S.S., Wilk, M.B., 1965. Analysis of variance test for normality (complete samples). Biometrika 52 (3/4), 591–611.
Sierpowska, J., Gabarrós, A., Fernandez-Coello, A., Camins, À., Castañer, S., Juncadella, M., de Diego-Balaguer, R., Rodríguez-Fornells, A., 2015. Morphological derivation overflow as a result of disruption of the left frontal aslant white matter tract. Brain Lang. 142, 54–64.
Tarantino, V., De Sanctis, T., Straulino, E., Begliomini, C., Castiello, U., 2014. Object size modulate sfronto-parietal activity during reaching movements. Eur. J. Neurosci. 39 (9), 1528–1537.
Thiebaut de Schotten, M., Dell'Acqua, F., Valabregue, R., Catani, M., 2012. Monkey to human comparative anatomy of the frontal lobe association tracts. Cortex. 48 (1), 82–96.
Tomassini, V., Jbabdi, S., Klein, J.C., Behrens, T.E., Pozzilli, C., Matthews, P.M., Rushworth, M.F., Johansen-Berg, H., 2007. Diffusion-weighted imaging tractography-based parcellation of the human lateral premotor cortex identifies dorsal and ventral subregions with anatomical and functional specializations. J. Neurosci. 27 (38), 10259–10269.
Tournier, J.D., Calamante, F., Gadian, D.G., Connelly, A., 2004. Direct estimation of the fiber orientation density function from diffusion-weighted MRI data using spherical deconvolution. Neuroimage 23 (3), 1176–1185.
Tournier, J.D., Calamante, F., Connelly, A., 2007. Robust determination of the fibre orientation distribution in diffusion MRI: non-negativity constrained super-resolved spherical deconvolution. Neuroimage 35 (4), 1459–1472.
Tretriluxana, J., Gordon, J., Winstein, C.J., 2008. Manual asymmetries in grasp-shaping and transport-grasp coordination. Exp. Brain Res. 188 (2), 205–315.
Vassal, F., Boutet, C., Lemaire, J.J., Nuti, C., 2014. New insights into the functional significance of the frontal aslant tract—An anatomo–functional study using intraoperative electrical stimulations combined with diffusion tensor imaging-based fiber tracking. Br. J. Neurosurg. 28 (5), 685–687.
Vergani, F., Lacerda, L., Martino, J., Attems, J., Morris, C., Mitchell, P., Thiebaut de Schotten, M., Dell'Acqua, F., 2014. White matter connections of the supplementary motor area in humans. J. Neurol. Neurosurg. Psychiatry 85 (12), 1377–1385.
Vogt, O., Vogt, C., 1919. Ergebnisse unserer Hirnforschung. J. Psychol. Neurol. 25, 277–462.
Wang, R., Benner, T., Sorensen, A.G., Wedeen, V.J., 2007. Diffusion Toolkit: a software package for diffusion imaging data processing and tractography. Proc. Int. Soc. Mag. Reson. Med. 15, 3720.
Winstein, C.J., Pohl, P.S., 1995. Effects of unilateral brain damage on the control of goal-directed hand movements. Exp. Brain Res. 105 (1), 163–174.